Pergamon

Geochimica et Cosmochimica Acta, Vol. 67, No. 3, pp. 413–419, 2003

0016-7037/03 $22.00 + .00

PII S0016-7037(00)01137-7

Selenium isotope fractionation during reduction by Fe(II)-Fe(III) hydroxide-sulfate (green rust)

THOMAS M. JOHNSON[1,*] and THOMAS D. BULLEN[2]

[1]Department of Geology, 245 Natural History Building, MC-102, University of Illinois, Urbana-Champaign, Urbana, IL 61820, USA
[2]Water Resources Division, U.S. Geological Survey, 345 Middlefield Road, Menlo Park, CA 94025, USA

(*Received February* 28, 2001; *accepted in revised form July* 30, 2002)

Abstract—We have determined the extent of Se isotope fractionation induced by reduction of selenate by sulfate interlayered green rust (GR_{SO_4}), a Fe(II)-Fe(III) hydroxide-sulfate. This compound is known to reduce selenate to Se(0), and it is the only naturally relevant abiotic selenate reduction pathway documented to date. Se reduction reactions, when they occur in nature, greatly reduce Se mobility and bioavailability. Se stable isotope analysis shows promise as an indicator of Se reduction, and Se isotope fractionation by various Se reactions must be known in order to refine this tool. We measured the increase in the $^{80}Se/^{76}Se$ ratio of dissolved selenate as lighter isotopes were preferentially consumed during reduction by GR_{SO_4}. Six different experiments that used GR_{SO_4} made by two methods, with varying solution compositions and pH, yielded identical isotopic fractionations. Regression of all the data yielded an instantaneous isotope fractionation of $7.36 \pm 0.24‰$. Selenate reduction by GR_{SO_4} induces much greater isotopic fractionation than does bacterial selenate reduction. If selenate reduction by GR_{SO_4} occurs in nature, it may be identifiable on the basis of its relatively large isotopic fractionation. *Copyright © 2003 Elsevier Science Ltd*

1. INTRODUCTION

Understanding and predicting the transport, cycling, and bioavailability of selenium, a potentially toxic and otherwise geochemically significant element, is difficult because of the complexity of selenium geochemistry. Se can be found in (VI), (IV), (0), and (-II) valences and in a variety of organic compounds (Elrashidi et al., 1987; McNeal and Balistrieri, 1989). Redox disequilibrium among the Se species is typically observed, and many of the redox reactions are thought to be microbially mediated (Oremland, 1994; White and Dubrovsky, 1994). Se(VI) and Se(IV) oxyanions are highly soluble, although Se(IV) adsorbs to solids more strongly at near-neutral pH (e.g., Bar-Yosef and Meek, 1987). Because Se(0), or elemental Se, is insoluble, reduction of the oxyanions reduces the mobility and bioavailability of Se. In the arid environments where agriculture-related Se contamination occurs, Se(VI) is the dominant species (e.g., Presser, 1994), whereas in the oceans and other aqueous environments, Se(VI), Se(IV), or organically bound Se may be the most abundant dissolved species (e.g., Cutter and Bruland, 1984).

Se stable isotopes can aid in geochemical studies, either as a tracer of Se sources or as an indicator of biogeochemical processes. The six stable isotopes, ^{74}Se, ^{76}Se, ^{77}Se, ^{78}Se, ^{80}Se, and ^{82}Se, are present in abundances of 0.89, 9.34, 7.64, 23.77, 49.61, and 8.73%. Se oxyanion reduction, either bacterial or abiotic, involves an enrichment of lighter isotopes in the reaction products and a complementary enrichment of the heavier isotopes in the remaining unreduced Se (Krouse and Thode, 1962; Rees and Thode, 1966; Rashid and Krouse, 1985; Herbel et al., 2000; Ellis et al., 2002). This is the dominant cause of Se isotope ratio variation in nature, and isotope ratio shifts are thus useful as an indicator of reduction (Johnson et al., 2000). However, all of the important Se reactions must be studied isotopically to allow unequivocal interpretation of data from natural environments. It is particularly important that all of the relevant Se oxyanion reduction reactions be studied because these are most likely to induce significant fractionation.

Although microbial action is reported to be an important, and likely dominant, Se oxyanion reduction pathway (e.g., Oremland et al., 1994; Blum et al., 1998), recent research has identified abiotic reduction of Se(VI) by sulfate interlayered green rust and proposed that it too may be important in nature (Myneni et al., 1997). This compound has the chemical formula $Fe(II)_4Fe(III)_2(OH)_{12}SO_4 \cdot 3H_2O$ and is given the abbreviation GR_{SO_4} (Hansen et al., 1994). Selenate reduction by GR_{SO_4} is significant because reduction of selenate by many reducing agents, including BH_4^- (Dedina and Tsalev, 1995) and Fe(II) (Myneni et al., 1997), is kinetically inhibited in the solution phase at earth surface temperatures. GR_{SO_4} has an unusual crystal structure, with positively charged oxide layers that create interlayer sites where anions such as SO_4^{2-} and SeO_4^{2-} are loosely bonded and readily exchanged with the surrounding solution. Presumably, when $SeO_4^{=}$ is reduced by green rust, it is taken into these sites, then reduced via electron transfer from Fe(II) in the crystal lattice. Because this is a potentially important reduction mechanism in nature, the isotopic fractionation involved must be measured. Furthermore, if this fractionation is systematically different from that induced by microbes, the potential exists to distinguish microbial reduction from that induced by GR_{SO_4}. In this article, we present measurements of Se isotope fractionation during reduction of selenate by GR_{SO_4}, compare this to previous knowledge of Se isotope systematics, and discuss the implications for application of Se isotopes measurements.

2. EXPERIMENTAL METHODS

2.1. Generation of Green Rust

Experiments were conducted, and reagents were stored, in 125-mL glass serum bottles, with crimp-sealed gray butyl stoppers and positive-

* Author to whom correspondence should be addressed (tmjohnsn@uiuc.edu).

Table 1. Experimental conditions and results.

Experiment	Initial pH	Final pH	GR_{SO_4} (mM)	Fe(II) (mM)	SO_4^{2-} (mM)	Na^+ (mM)	Cl^- (mM)	Half-life[a] (h)	ε^b (‰)	n
GR37	7.0	6.0	0.41	0.50	3.7	6.5	0.0	20	−7.34 ± 0.4	3
GR39	7.0	5.9	0.41	0.16	1.1	1.8	0.0	2.9	−7.35 ± 0.2	5
GR40	6.9	5.9	0.41	0.24	2.0	3.4	0.0	4.3	−7.24 ± 0.2	4
GR33	6.8	6.8	0.80	1.20	7.2	13.0	0.0	11	−7.43 ± 0.3	4
GR10	7.3	7.3	0.67	0.17	2.1	6.8	2.12	15	−7.22 ± 0.4	4
GR09	6.2	6.3	0.48	0.28	1.6	3.7	0.99	7.9	−7.57 ± 0.4	3

[a] Selenate half-life was derived by fitting data to a first-order reaction model.
[b] Uncertainties are two standard errors derived from regression.

pressure N_2 headspaces. Sampling and transfer of reagents was done via N_2-flushed syringes and needles inserted through the septa. Before solutions were withdrawn, N_2 was injected to compensate for the removed volumes. Dissolved O_2 in water or reagent solutions was removed by bubbling high-purity N_2 through the septum bottles for 20 min.

GR_{SO_4} was synthesized by a base titration method (Hansen et al., 1994; Myneni et al., 1997) for experiments GR09 and GR10 and an oxidation method (Refait et al., 1999) for the others. For the base titration method, a 47 mM Fe(II) stock solution was made by dissolving 1.39 g reagent-grade $FeSO_4 \cdot 7H_2O$ crystals in 100 mL O_2-free deionized water. The solution was transferred to a serum bottle, and the headspace was thoroughly flushed with N_2. Although the reagent was newly purchased, a significant fraction of the Fe(II) had oxidized to Fe(III). This was removed from the solution by precipitation. A few milliliters of 1.0 mol/L NaOH were added to attain a pH between 6.5 and 7. A green rust precipitate formed and removed the Fe(III) contaminant from solution. This precipitate was removed from the bottle, and the Fe concentration of the remaining stock solution was measured. A 0.2 M Fe(III) solution was made by dissolving 2.7g $FeCl_3 \cdot 6H_2O$ in 50 mL water.

Formation of GR_{SO_4} by the base titration method followed previously published studies (Hansen et al., 1994; Myneni et al., 1997). Fe(II)SO_4 solution was transferred from the stock bottle via a syringe and injected into ~100 mL O_2-free deionized water. The volume of injected Fe(II)SO_4 solution was selected to attain the GR_{SO_4} suspension strengths given in Table 1. Fe(III)Cl_3 stock solution was injected to attain a Fe(II):Fe(III) molar ratio of 2.5:1. This is intentionally greater than the stoichiometric ratio for green rust formation. Accidental injection of small amounts of O_2 converted some of the Fe(II) to Fe(III), and the excess Fe(II) ensured that no ferrihydrite precipitate persisted after green rust precipitation. GR_{SO_4} precipitates were formed by slowly adding 0.1 M NaOH to attain pH values close to neutral. During this addition, a yellowish ferrihydrite precipitate formed first, followed by a reaction starting at about pH 5.5 that consumed the ferrihydrite and formed a bluish-green-colored GR_{SO_4} precipitate (Hansen et al., 1994). In the present study, Cl^- was present in solution (Table 1), but very little substitution of Cl^- for $SO_4^=$ occurs under these conditions. This is because divalent anions are strongly preferred by GR_{SO_4} in the interlayer sites (Miyata, 1983).

Formation of GR_{SO_4} by the oxidation method followed procedures of a recently published study (Refait et al., 1999). A solution of 100 mM $FeSO_4$ + 50 mM H_2SO_4 was made by reacting 150 mM H_2SO_4 with Fe^0 (Hansen et al., 1994) in a gently warmed serum bottle with a needle piercing the septum to release evolved H_2. A total of 50 mL of this solution was mixed with 50 mL 250 mM NaOH in an anaerobic serum bottle; then additional 250 mM NaOH was added until a colorless $Fe(OH)_2$ precipitate formed, and the aqueous Fe(II) concentration decreased to ~12 mM. The $Fe(OH)_2$ suspension was then oxidized by exposure to air in an open beaker stirred moderately with a magnetic stirring bar. GR_{SO_4} formed, and the suspension turned a deep bluish-green color. After about 1 h, GR_{SO_4} formation was complete, as indicated by an abrupt change from a reaction-buffered pH of ~7.8 to a reaction-buffered pH of 6.8. This stock suspension, which contained 7 mM GR_{SO_4}, 8.5 mM Fe(II), and 65 mM SO_4^{2-}, was stored in an anaerobic septum bottle. Suspensions for experiments GR33, GR37, GR39, and GR40 were created by injecting aliquots of the stock into septum bottles containing degassed, deionized water. In experiments GR39 and GR40, the stock aliquots were centrifuged before injection and approximately 75% of the supernatant was removed from the suspension before it was injected. This resulted in lower concentrations of dissolved Fe, sulfate, and Na than in experiments GR33 and GR37.

Samples of GR_{SO_4} produced by both methods were analyzed for Fe(II), Fe(III), and S contents. Aliquots of the suspensions were filtered under N_2 and rinsed with 0.1 mol/L NaCl. The filters were immediately immersed in 10 mL O_2-free 0.4 mol/L HCl under N_2 to dissolve the green rust. These solutions were diluted with O_2-free deionized water and analyzed for Fe(II), total dissolved Fe, and S concentrations by means of the methods given below. The green rust samples were found to be within 10% of the expected 4:2:1 Fe(II):Fe(III):S ratio.

X-ray diffraction was used to confirm the identity of a sample of GR_{SO_4} produced by the oxidation method. A sample of the suspension was injected into a 0.4-mm–inner diameter glass capillary, which was then flame sealed. The green rust was concentrated in one end of the capillary by centrifugation, and a powder diffraction pattern (Fig. 1) was obtained with a Bruker P4 diffractometer with a rotating anode Cu-Kα source. The great intensity of this source allowed use of Cu-Kα radiation, which is normally limited with Fe-rich compounds. A blank capillary, containing the solution but not the green rust, was analyzed to obtain a background spectrum, which was subtracted from the raw GR_{SO_4} spectrum. The d spacings calculated from the diffraction pattern match those given by Hansen et al. (1994) (Table 2). A small amount of ferrihydrite is also present, as indicated by an additional reflection at 36.5° (d = 0.245 nm).

2.2. Se Addition, Sampling, and Concentration Analysis

The compositions of the GR_{SO_4} suspensions are given in Table 1. Selenate (as 1 mM Na_2SeO_4 solution) was injected into each suspension to attain a starting concentration of ~0.030 mM Se. Initial con-

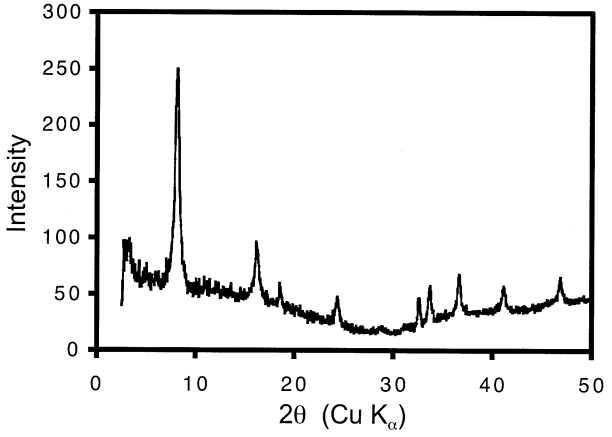

Fig. 1. X-ray diffraction pattern obtained for GR_{SO_4} produced by the oxidation method.

Table 2. Measured vs. published X-ray diffraction data.

2 θ	hkl	d (nm)	d (nm) Hansen et al. (1994)
8.110	003	1.0919	1.103
16.212	006	0.5476	0.549
24.345	009	0.3662	0.3657
32.566	101	0.2754	0.2751
33.640	013	0.2668	0.2668
41.101	019	0.2200	0.2200
46.832	1012	0.1943	0.1958

centrations of Se (Table 3) were calculated from the masses of the suspensions and the added Se stock solutions, and the measured concentration of the stock. The suspensions were at least 0.41 mM GR_{SO_4} and contained enough Fe(II) to reduce at least four times the injected amount of Se to Se(0).

Experiments were conducted with Se(IV) in similar fashion (Fig. 2). Se(IV) (as 1 mM Na_2SeO_3 solution) was added to attain starting concentrations of ~0.030 mM Se. In these experiments, adsorption was a significant problem; Se(IV) adsorption is strong at circumneutral pH

Table 3. Se concentration and isotope data.

Experiment	Time elapsed (h)	[Se] (μM)	$\delta^{80/76}$Se (‰)
GR37	0.0	23.8[a]	2.25[b]
	0.9	23.8	—
	10.9	24.2	2.36
	18.9	18.2	4.22
	42.4	8.1	10.46
			10.53[c]
	66.0	0.0	—
GR39	0.0	22.6[a]	2.25[b]
	0.5	20.5	1.99
	3.5	17.4	2.91
	6.5	12.0	5.50
	9.8	7.2	9.80
			9.92[c]
	19.8	0.4	30.86
	24.8	0.0	—
GR40	0.0	24.9[a]	2.25[b]
	1.6	23.2	—
	6.1	19.2	3.93
	9.3	11.1	7.90
	19.3	0.5	29.53
	24.3	0.0	—
GR33	0.0	22.2[a]	2.25[b]
	0.5	21.1	2.38
	5.0	19.7	—
	10.5	19.5	2.89
	53.0	1.7	21.15
	60.0	0.8	25.94
GR10	0.0	33.3[a]	2.25[b]
	0.1	31.6	2.30
	29.0	7.5	13.26
	37.3	5.3	16.71
	56.7	2.4	20.53
GR09	0.0	33.3[a]	2.25[b]
	0.1	32.8	—
	24.8	10.8	10.42
			10.26[c]
	43.8	2.0	23.35

[a] Calculated from mass Se stock injected.
[b] Known value of injected Se stock solution.
[c] Duplicate analysis.

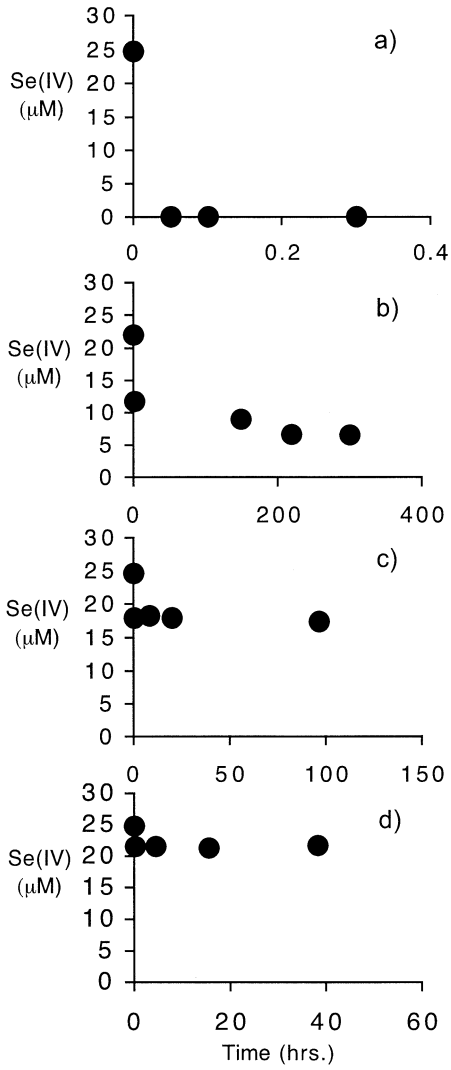

Fig. 2. Evolution of Se(IV) concentration during reaction with 0.4 mM green rust suspensions with (a) 0.0 mM, (b) 0.11 mM, (c) 0.63 mM, and (d) 1.1 mM $HPO_4^{2-}/H_2PO_4^-$.

(Bar-Yosef and Meek, 1987). In an attempt to decrease adsorption enough to measure the progress of reduction, small amounts of a 1.0 M pH 7 $HPO_4^{2-}/H_2PO_4^-$ solution were added just before Se injection in some of the Se(IV) experiments. Initial $HPO_4^{2-}/H_2PO_4^-$ concentrations ranged from 0.1 to 1.9 mM.

The bottles were placed on a shaker table to keep the GR_{SO_4} completely suspended. As Se reduction proceeded, the GR_{SO_4} changed color gradually from bluish green to gray to black. Samples of the well-mixed suspensions were withdrawn periodically with a syringe; the removed volume was replaced by N_2. Samples were filtered within 1 min, acidified with 0.1 mL 6 M HCl/5 mL of sample, and stored in screw-top polypropylene centrifuge tubes.

Se concentration measurements were obtained via hydride generation atomic absorption spectrometry (Dedina and Tsalev, 1995). Se(IV) was measured by diluting a subsample 1:100 with 4 M HCl, generating H_2Se with a Varian VGA-76 hydride generator and measuring absorption with a Perkin-Elmer 3030 AA spectrophotometer. Total Se (VI + IV) was determined via the same procedure, except the diluted subsample was heated at 100°C for 60 min to convert Se(VI) to Se(IV) before measurement. Uncertainty for the Se concentration measurements was $\pm 10\%$ (2σ), according to results of replicate measurements and standard additions. Fe analyses were obtained by the ferrozine

colorimetric method (Viollier et al., 2000) with a Spectronic Genesys 20 visible light spectrometer operating at 562 nm. S analyses were obtained by inductively coupled plasma atomic emission spectrometry with a Perkin-Elmer Optima 2000 DV instrument. Na and Cl concentrations were calculated from the known amounts of NaOH, HCl, and $FeCl_3$ solutions added in the experiments. Fe, S, Na, and Cl determinations were precise to ±5%.

2.3. Isotope Ratio Measurements

Procedures for isotope ratio measurement followed those presented in previous studies (Johnson et al., 1999); they are briefly reviewed here. A double isotope spike method is used to correct for isotopic fractionation occurring during sample preparation and mass spectrometry. A subsample is taken and a "double spike" solution, containing ^{74}Se and ^{82}Se in the same chemical form as the sample Se, is added and thoroughly mixed with it. Se is purified for mass spectrometry using hydride generation via a continuous flow system that reacts the sample, in a 6 M HCl matrix, with a 1% $NaBH_4$ solution to produce H_2Se and recovers the Se in a concentrated HNO_3 trap (Ellis et al., 2002). The HNO_3 is evaporated to dryness, and any organic residue is oxidixed with H_2O_2. Negative-ion thermal ionization mass spectrometry is used to measure the isotope ratios. A total of 0.5 μg of the purified Se is loaded onto a Re filament with colloidal graphite and $Ba(OH)_2$ (Johnson et al., 1999). Optimal ionization temperatures were approximately 960°C. $^{82}Se/^{80}Se$, $^{80}Se/^{76}Se$, and $^{76}Se/^{74}Se$ were measured in sequence, with a total of 50 measurement cycles providing opportunity to assess internal precision and discard outliers. The measured $^{82}Se/^{74}Se$ ratio was used to correct for isotopic fractionation occurring during sample preparation and mass spectrometry. The $^{80}Se/^{76}Se$ of the sample, with the double spike mathematically removed and the analytical isotopic fractionation corrected for, was extracted from the data via an iterative data reduction routine (Johnson et al., 1999). The precision of this method is ±0.2‰, according to measurements of duplicate sample preparations and standards. Duplicate analyses are presented in Table 3.

Results are expressed in terms of delta notation,

$$\delta^{80/76}\mathrm{Se} = \frac{\mathrm{R_{meas}} - \mathrm{R_{std}}}{\mathrm{R_{std}}} \times 1000‰ \quad (1)$$

where R_{meas} and R_{std} are the $^{80}Se/^{76}Se$ of the measured sample and the standard, respectively. The standard used in this study is the MH495 standard, which is −2.3‰ relative to Se from Canyon Diablo troilite. This is an intralaboratory standard because no interlaboratory standards exist yet.

3. RESULTS

3.1. Evolution of Experiments

In the selenate reduction experiments, green rust reduced selenate and removed it from solution as observed in the previous study (Myneni et al., 1997). Selenate concentrations as a function of time are given in Table 3 and Figure 3. No dissolved Se(IV) was detected in these experiments, indicating that the evolved Se(IV) was completely adsorbed and/or rapidly reduced to insoluble Se(0). A lag was observed in some experiments; selenate concentrations decreased slowly or were constant for the first 2 to 10 h (see discussion). After that, the observed decreases are roughly consistent with first-order reaction kinetics, with half-lives ranging from 2.9 to 20 h (Table 1). These rates are 3 to 20 times faster than those reported by Myneni et al. (1997). Experiments with lesser sulfate concentrations generally had greater reaction rates, presumably because selenate ions had less competition from sulfate and thus had more frequent contact with the reduction sites within the green rust. Initial pH values in the experiments ranged from 6.3 to 7.3. In the three experiments with the lowest green rust concentrations, pH dropped near the end of the experiments to roughly 6.0 (Table 1). In the other experiments, no significant pH change was observed.

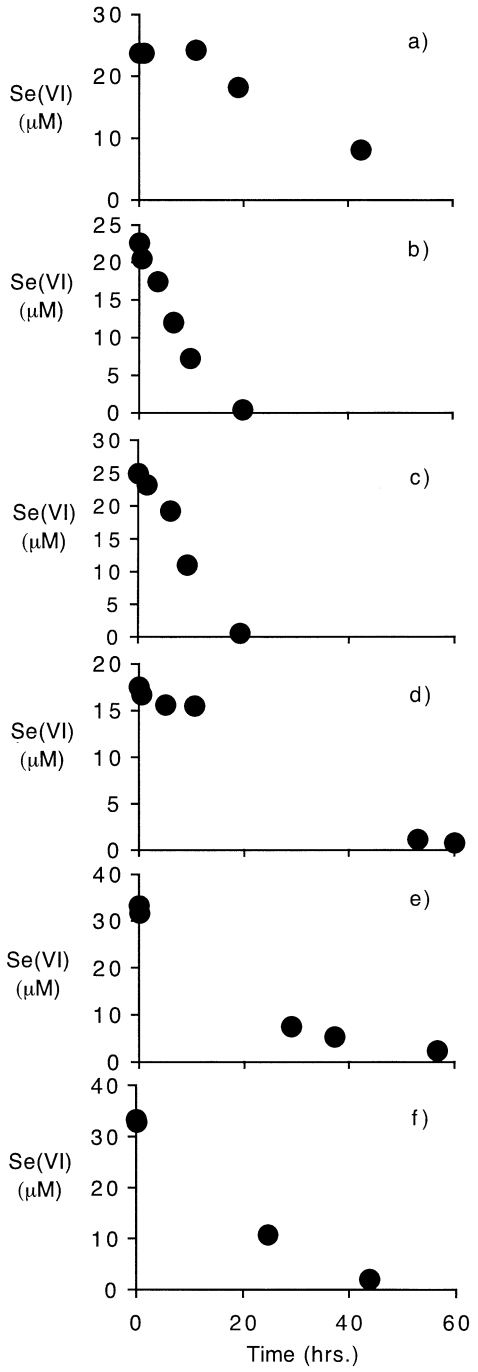

Fig. 3. Evolution of Se(VI) concentration during experiments (a) GR37, (b) GR39, (c) GR40, (d) GR33, (e) GR10, and (f) GR09.

Myneni et al. (1997) detected rapid reduction, by green rust, of Se(IV) produced by reduction of Se(VI) in the interior of green rust crystals. That work was done with X-ray spectroscopy. With our methods, it was not possible to separate reduction from adsorption. In an experiment in which no $HPO_4^{2-}/H_2PO_4^-$ solution was added to retard adsorption, dissolved

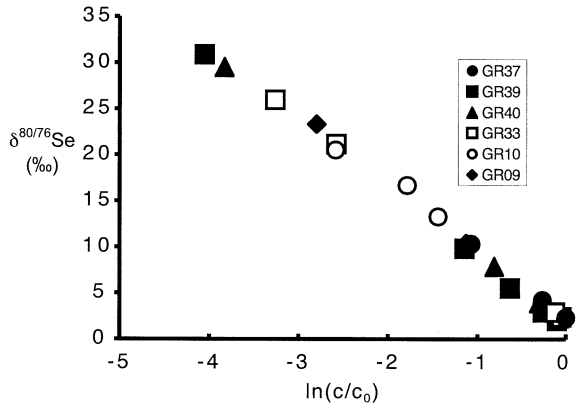

Fig. 4. Se isotope ratio data from all selenate reduction experiments plotted against $\ln(c/c_0)$, the natural logarithm of the fraction of unreduced Se remaining. The slope of the line gives ε. Uncertainty in $\ln(c/c_0)$ is approximately the width of the symbols. Uncertainty in $\delta^{80/76}$Se is ± 0.2‰, much smaller than the symbols.

Se(IV) concentration decreased rapidly and was zero in less than 20 min (Fig. 2). Adsorption and reduction probably occurred simultaneously, but it is not possible to determine accurately, with the methods available in this study, how much of the dissolved Se(IV) loss was caused by reduction. However, in an experiment with 0.1 mM $HPO_4^{2-}/H_2PO_4^-$ 47% of the added Se(IV) was adsorbed (Fig. 2). In the experiment without $HPO_4^{2-}/H_2PO_4^-$, adsorption must have been much greater than 47% and could have caused all the removal from solution observed. In several experiments with 1 to 2 mM $HPO_4^{2-}/H_2PO_4^-$ (Fig. 2), less than 13% of the Se(IV) was adsorbed, and this enabled an assessment of Se(IV) reduction. However, Se(IV) reduction was nonexistent or extremely slow (Fig. 2). It appears that blocking adsorption with competing anions results in severe inhibition of Se(IV) reduction. No further work with Se(IV) reduction was conducted, as Se(IV) reduction by GR_{SO_4} is much less important than Se(VI) reduction by GR_{SO_4} (see discussion).

3.2. Isotope Ratio Results

In the selenate reduction experiments, as dissolved Se concentrations decreased, $\delta^{80/76}$Se values of the remaining dissolved Se increased (Table 3; Fig. 4). The lighter Se isotopes were preferentially removed from solution via reduction, as is observed with all other Se oxyanion reduction reactions, both microbial and abiotic. This is a kinetic isotope effect; the reaction proceeds to completion with no back reaction. The size of this kinetic isotope effect can be determined by fitting the data to a Rayleigh distillation model, which assumes that selenate removed from solution by reduction is removed permanently (i.e., no back-reaction occurs).

Assuming a Rayleigh process in which the $\delta^{80/76}$Se of the reduced Se produced at any instant is shifted from that of the unreduced pool by a constant per mil value, $^{80}Se/^{76}Se$ ratios in the dissolved selenate evolve according to

$$\delta_{rem} = \delta_0 + \varepsilon \times \ln(c/c_0) \quad (2)$$

where ε is the isotopic shift (‰) induced by the reaction, c and c_0 are the dissolved selenate concentrations at the time of sampling and initially, δ_{rem} is the $\delta^{80/76}$Se value of the unreduced pool as it changes with time, and δ_0 is the initial $\delta^{80/76}$Se value of the injected Se. Specifically, ε is given by

$$\varepsilon = \delta_{product} - \delta_{rem} \quad (3)$$

where $\delta_{product}$ gives the isotopic composition of the reaction product produced at one instant in time and δ_{rem} gives the isotopic composition of the reactant pool at that instant. More generally, the slope of a line on a δ_{rem} vs. $\ln(c/c_0)$ plot is equal to ε, even if the slope is not constant as a function of $\ln(c/c_0)$ (Herbel et al., 2000).

In Figure 4, $\delta^{80/76}$Se data are plotted vs. $\ln(c/c_0)$ for all experiments. Plots for individual experiments are straight lines within the uncertainties, and thus ε was invariant over time as reduction proceeded. Values of ε for individual experiments are given in Table 1. Because the relative uncertainty of the concentration measurements was much greater than that of the isotope determinations, these data were analyzed by means of linear regression with $\ln(c/c_0)$ as the y variable. All of the experiments are consistent with a single value of ε; the slope of the best fit straight line through the data, is -7.36‰, with a 2σ uncertainty of 0.24‰. The standard error in $\ln(c/c_0)$ calculated for the regression was 0.09. This $\sim$1.8 times larger than can be explained by the uncertainty in the Se concentration measurements, but there is no clear correlation of residuals with experimental parameters.

The experiments reported here had an initial pH range of 6.3 to 7.3, and in three of them, the pH dropped from roughly 7.0 to roughly 6.0 at or near the time selenate reduction was complete. There is no correlation between pH and isotopic fractionation in this range. Similarly, no correlation exists between ε and reaction rate, dissolved Fe(II), sulfate, Na^+, or Cl^- concentrations.

4. DISCUSSION

4.1. Comparison to Previous Abiotic Reduction Experiments

The only previous study of Se isotope fractionation during room-temperature, abiotic Se(VI) reduction (Rees and Thode, 1966) used 8 M HCl as the reductant, and the results indicate an ε value of 12.0‰. This is much larger than the ε value determined for GR_{SO_4} in the present study. This difference can be understood in terms of differences in the reduction processes. In the sulfur isotope literature (e.g., Rees, 1973), modeling of kinetic S isotope fractionation during sulfate reduction assumes fractionation is caused mainly by S-O bond breakage, which has a fundamental tendency to favor lighter isotopes. We assume, by analogy, that Se isotope fractionation during selenate reduction is driven by Se-O bond breakage. However, if there are multiple steps in the overall reduction process, the overall kinetic isotope effect depends on these steps as well. The green rust reduction process consists of a diffusion step followed by a reduction step. Because the green rust structure consists of positively charged layers with exchangeable interlayer anions, the vast majority of the sites for Se(VI) reduction should be on interior interlayer surface sites. The reduction

sites are not in direct communication with the bulk solution; a diffusive barrier exists between solution and interlayer spaces.

The overall isotopic fractionation between the Se(VI) in the bulk solution and the Se(IV) produced by reduction is expected to be less than that occurring during the Se-O bond rupture at the reduction sites. This is because the Se(VI) in interlayer spaces becomes somewhat enriched in the heavier isotopes as the lighter isotopes are preferentially reduced. The degree to which this happens depends on the rate of diffusive exchange relative to the reduction rate. If the diffusion rate substantially limits the overall reaction rate, then the isotopic fractionation for the overall reaction will be less than that occurring during the reduction step. The results of Myneni et al. (1997) suggest that diffusion does indeed limit the reaction rate; Se(VI) reduction was much faster when the selenate was coprecipitated within green rust than when it was added to the solution after formation of the green rust. Thus, the difference in isotopic fractionation between the green rust experiments and the HCl experiments is consistent with basic isotopic systematics.

4.2. Comparison of Green Rust and Bacterial Results

The Se isotope fractionation in the selenate reduction experiments is larger than that measured for microbial selenate reduction. Pure culture experiments with *Sulfurospirillum barnesii* and *Bacillus arsenicoselenatis* (Herbel et al., 2000) revealed a range of ε with a maximum value of 5.0‰. In these experiments, ε depended on experimental conditions. This has been observed with sulfur isotope fractionation during sulfate reduction, where ε has been correlated with reaction rate and/or electron donor type (Kaplan and Rittenberg, 1964; Habicht and Canfield, 1997; Brüchert et al., 2001). More importantly, sediment slurry experiments in which selenate reduction was mediated by microbes under nearly natural conditions revealed a narrow range of ε, -2.6 to -3.1‰, with sediments from three different sites (Ellis et al., 2002). In those experiments, sediments from an estuarine tidal flat, a Se-contaminated agricultural wastewater canal, and an artificial wetland designed to remove selenate from wastewater were incubated anaerobically without any added electron donors or nutrients. The sediments were disturbed by homogenization and were shaken constantly during the experiments, but otherwise the microbes and nutrients were completely natural. Accordingly, these slurry experiments give the best estimate, at present, for the value of ε in wetland environments. In comparison, the ε values for reduction by green rust are more than twice as large. They are more than 40% greater than the largest values observed in the pure culture experiments. This result is similar to that observed with sulfate reduction, where microbial isotope fractionation is generally less than abiotic sulfate reduction (Kaplan and Rittenberg, 1964; Habicht and Canfield, 1997).

It may be possible to use this contrast in isotopic fractionation to distinguish between microbially mediated and GR_{SO_4}-induced reduction. For example, if a $\delta^{80/76}$Se difference of 7‰ were observed between dissolved Se(VI) and adsorbed Se(IV) in a groundwater system, green rust reduction would be a likely candidate for the dominant reduction process. On the other hand, other abiotic selenate reduction processes may yet be discovered, and these may also induce isotope effects that are larger than those induced by microbes.

4.3. Details of the Reduction Process

A lag of approximately 10 h was observed at the beginning of some of the experiments; selenate reduction was very slow or did not occur (Fig. 3). Either the selenate did not attain full contact immediately with the reactive sites in the green rust structure, or exposure to selenate changed the green rust during this 10-h period. Simple aging of the green rust cannot explain the lag, which occurred consistently in several experiments, including some not shown here, with green rust aged 1 d to several weeks after synthesis. Also, microbial action cannot be involved, even though the experiments were not sterilized. The reaction rates here are similar to those observed in culturing experiments with optimal, nutrient-rich media and inoculants of known selenate reducers. In our experiments, highly reproducible, rapid reduction was observed with no nutrients and no inoculants, and it is inconceivable that microbes could multiply and flourish in such a short amount of time with essentially no nutrients. Additionally, the observed lag cannot be related to the time needed for selenate to substitute for sulfate in the green rust interlayer sites. A simple diffusive lag would be present throughout the experiments and reaction rates would not increase after 10 h. Thus, we conclude that slow reduction in the first hours of the experiments alters the green rust in some way, perhaps through oxidative damage to the crystal structure, that increases its reactivity.

Our analysis assumes that the observed decreases in selenate concentration are solely due to selenate reduction, and not adsorption onto green rust surfaces. This assumption is supported by both observations from the experiments and theoretical considerations. First, we expect adsorption onto outer surfaces to reach equilibrium within minutes, and measured selenate concentrations do not indicate significant losses from solution in the first minutes of the experiments. In experiments GR09, GR10, GR33, and GR37, selenate concentrations measured in the first hour after injection of selenate were within 5% of the amount calculated from the mass and concentration of the added Se stock solution (Fig. 3; Table 3). In GR39 and GR40, decreases of 7 and 10% occurred but are due to the rapid reduction. Second, the molar ratio of sulfate to selenate in these experiments ranged from 35 to 240. Assuming equal competition of selenate and sulfate for adsorption sites, only a small fraction of the sites would be occupied by selenate. A small amount of selenate adsorption must have occurred, and is suggested by the plots in Figure 3, but was within the analytical uncertainties and does not affect our data analysis significantly.

4.4. Se(IV) Reduction by Green Rust

Reduction of selenate by GR_{SO_4} may be important in natural systems, but reduction of Se(IV) by green rust is less important. Green rust is the only reported naturally occurring abiotic reductant of selenate under naturally relevant conditions. In contrast, Se(IV) reduction is less inhibited kinetically, and is induced by a variety of abiotic and bacterial processes (McNeal and Balistrieri, 1989). Furthermore, adsorption is a major removal mechanism for Se(IV), and thus reduction is not necessarily the dominant removal process as is the case with Se(VI).

5. CONCLUSIONS

When GR_{SO_4} reduces selenate, lighter Se isotopes are enriched in the reaction products; the $^{80}Se/^{76}Se$ ratio is shifted by $7.36 \pm 0.24‰$. This Se isotope fractionation, ε, is larger than that induced by microbial Se(VI) reduction, and $\delta^{80/76}Se$ differences between selenate and reduced Se may thus be useful to determine which Se(VI) reduction mechanism dominates in field settings. More generally, the results of this study are important when Se isotope ratios are used to indicate selenate reduction. The degree of heavier isotope enrichment in dissolved selenate can be used to determine the amount of selenate reduction that has occurred in an aqueous system, but only if the size of the isotopic fractionation is known. Our results indicate that ε depends on the reaction mechanism, with smaller values for microbial reduction and a greater value for green rust reduction.

Acknowledgments—This work was supported by the National Science Foundation, Division of Earth Sciences, Hydrological Sciences Program, under grants EAR 97-25799 and EAR 00-03381. We thank Mitch Herbel for performing some of the isotopic analyses. The article was improved through suggestions by David Cole, Satish Myneni, and two anonymous reviewers.

Associate editor: D. Cole

REFERENCES

Bar-Yosef B. and Meek D. (1987) Selenium sorption by kaolinite and montmorillonite. *Soil Sci.* **144,** 11–19.

Blum J. S., Bindi A. B., Buzzelli J., Stolz J., and Oremland R. S. (1998) *Bacillus arsenicoselenatis,* sp. nov., and *Bacillus selenitireducens,* sp. nov. Two haloalkaliphiles from Mono Lake, California that respire oxyanions of selenium and arsenic. *Arch. Microbiol.* **171,** 19–30.

Brüchert V., Knoblauch C., and Jørgensen B. B. (2001) Controls on stable sulfur isotope fractionation during bacterial sulfate reduction in Arctic sediments. *Geochim. Cosmochim. Acta* **65,** 763–776.

Cutter G. A. and Bruland K. W. (1984) The marine biogeochemistry of selenium: A re-evaluation. *Limnol. Oceanogr.* **29,** 1179–1192.

Dedina J. and Tsalev D. L. (1995) *Hydride Generation Atomic Absorption Spectrometry.* Wiley.

Ellis A. S., Johnson T. M., Bullen T. D., and Herbel M. J. (2003) Selenium isotope fractionation by natural microbial consortia in unamended sediment slurries. *Chem. Geol.*,in press.

Elrashidi M. A., Adriano D. C., Workman S. M., and Lindsay W. L. (1987) Chemical equilibria of selenium in soils; a theoretical development. *Soil Sci.* **144,** 141–152.

Habicht K. S. and Canfield D. E. (1997) Sulfur isotope fractionation during bacterial sulfate reduction in organic-rich sediments. *Geochim. Cosmochim. Acta* **61,** 5351–5361.

Hansen H. C. B., Borggaard O. K., and Sorensen J. (1994) Evaluation of the free energy of formation of Fe(II)-Fe(III) hydroxide-sulphate (green rust) and its reduction of nitrite. *Geochim. Cosmochim. Acta* **58,** 2599–2608.

Herbel M. J., Johnson T. M., Oremland R. S., and Bullen T. D. (2000) Selenium stable isotope fractionation during bacterial dissimilatory reduction of selenium oxyanions. *Geochim. Cosmochim. Acta* **64,** 3701–3709.

Johnson T. M., Herbel M. J., Bullen T. D., and Zawislanski P. T. (1999) Selenium isotope ratios as indicators of selenium sources and oxyanion reduction. *Geochim. Cosmochim. Acta* **63,** 2775–2783.

Johnson T. M., Bullen T. D., and Zawislanski P. T. (2000) Selenium stable isotope ratios as indicators of sources and cycling of selenium: Results from the northern reach of San Francisco Bay. *Environ. Sci. Technol.* **34,** 2075–2079.

Kaplan I. R. and Rittenberg S. C. (1964) Microbial fractionation of sulfur isotopes. *Gen. Microbiol.* **43,** 195–212.

Krouse H. R. and Thode H. C. (1962) Thermodynamic properties and geochemistry of isotopic compounds of selenium. *Can. J. Chem.* **40,** 367–375.

McNeal J. M. and Balistrieri L. S. (1989) Geochemistry and occurrence of selenium: An overview. In *Selenium in Agriculture and the Environment* (ed. L. W. Jacobs), pp. 1–13. Soil Science Society of America.

Miyata S. (1983) Anion exchange properties of hydrotalcite-like compounds. *Clays Clay Minerals* **31,** 305–311.

Myneni S. C. B., Tokunaga T. K., and Brown G. E. Jr. (1997) Abiotic selenium redox transformations in the presence of Fe(II,III) oxides. *Science* **278**(5340), 1106–1109.

Oremland R. S. (1994) Biogeochemical transformations of selenium in anoxic environments. In *Selenium in the Environment* (eds. W. T. Frankenberger and S. Benson), pp. 389–419. Marcel Dekker.

Oremland R. S., Blum J. S., Culbertson C. W., Visscher P. T., Miller L. G., Dowdle P., and Strohmaier F. E. (1994) Isolation, growth, and metabolism of an obligately anaerobic, selenate-respiring bacterium, strain SeS-3. *Appl. Environ. Microbiol.* **60,** 3011–3019.

Presser T. S. (1994) The Kesterson effect. *Environ. Manage.* **18,** 437–454.

Rashid K. and Krouse H. R. (1985) Selenium isotopic fractionation during SeO_3 reduction to Se^0 and H_2Se. *Can. J. Chem.* **63,** 3195–3199.

Rees C. E. (1973) A steady-state model for sulphur isotope fractionation in bacterial reduction processes. *Geochim. Cosmichim. Acta* **37,** 1141–1162.

Rees C. B. and Thode H. G. (1966) Selenium isotope effects in the reduction of sodium selenite and of sodium selenate. *Can. J. Chem.* **44,** 419–427.

Refait P., Bon C., Simon L., Bourrie G., Trolard F., Bessiere J., and Genin J. M. R. (1999) Chemical composition and Gibbs standard free energy of formation of Fe(II)-Fe(III) hydroxysulphate green rust and Fe(II) hydroxide. *Clay Minerals* **34,** 499–510.

Viollier E., Inglett P. W., Hunter K., Roychoudhury A. N., and Van Cappellen P. (2000) The ferrozine method revisited: Fe(II)Fe(III) determination in natural waters. *Appl. Geochem.* **15,** 785–790.

White A. F. and Dubrovsky N. M. (1994) Chemical oxidation-reduction controls on selenium mobility in groundwater systems. In *Selenium in the Environment* (eds. W. T. Frankenberger and S. Benson), pp. 185–221. Marcel Dekker.